Abstract

BACKGROUND. In Gram-negative bacteria, the outer-membrane represents an additional barrier antibiotics have to overcome to permeate inside pathogens. Our inability to come up with novel effective antibiotics mostly relies upon insufficient understanding of the molecular basis behind outer-membrane penetration.

RESULTS. Polar antibiotics can permeate through water-filled porins. Through molecular modeling, permeation of imipenem and meropenem through porins was found to strongly depend upon capability of drugs to properly align their electric dipole to the internal electric field in the restricted region of the pore. Electrostatics differences between OmpF and OmpC, and modifications along a series of OmpC mutants from *E. coli* resistant clinical strains identify a "pre-orientation" region, which dramatically affects antibiotic path. Electrostatics modifications along a series of porin mutants from resistant clinical strains identify a "pre-orientation" region, which dramatically affects antibiotic pathway.

CONCLUSIONS. A novel perspective is presented, suggesting new molecular properties to be included in drug design.

Keywords

Antimicrobial drugs, drug design, computational chemistry and molecular modelling

Introduction

Antimicrobial resistance (AMR) is a natural phenomenon in microorganisms. By a multitude of complex mechanisms, microorganisms develop resistance to the commonly employed antimicrobial drugs, meaning that they acquire the capability to grow and proliferate in the presence of chemicals that were previously able to limit their growth or even to kill them. AMR is accelerated by the selective pressure exerted by use and misuse of antimicrobial agents in humans and animals.

The lack of new classes of antimicrobials replacing those that have become ineffective, represents an additional problem. This issue is particularly urgent for Gram-negative pathogens [1–3]. A recent report published by the World Health Organization reads: “The pipeline for the development of new antibacterial drugs is now virtually empty, particularly for the treatment of Gram-negative enteric bacteria, and research on treatments to replace antibacterial drugs is still in the early stages. […] This means that progress in modern medicine, which relies on the availability of effective antibacterial drugs, is now at risk” [4].

In Gram-negative bacteria, the presence of an outer membrane (OM) represents an additional challenge, as the antibiotic has to overcome this barrier to permeate inside the pathogen. Beside the degradative action of devoted enzymes and the expulsion process operated by efflux pump systems, the accumulation of sufficient antibiotics inside the bacterial cell is of primary importance to have a significant effect [5,6]. Our inability to come up with novel effective antibiotics for Gram-negative pathogens mostly relies upon the insufficient understanding of the molecular basis behind penetration through the OM [7–9].

The latter consists of a lipopolysaccharides/phospholipids bilayer where water filled protein channels are embedded and serve to regulate nutrients uptake. More specifically, in the enterobacteriaceae (e.g. *Escherichia coli*), such a role is devolved to a family of trimeric non-specific channels called porins, through which metabolites and ions cross the OM by passive diffusion [6,10]. These outer membrane porins (Omp) represent also the main access to the periplasmic space of the bacterial cell for polar antibiotics from different classes, like β-lactams. One of the strategies used by pathogens to increase their resistance to drugs is to limit their uptake by modifying, indeed, the expression or the structure of porins [6,11].

E. coli is one of the most studied and well known Gram-negative bacteria and is usually taken as prototype. The two main porins of *E. coli* are not surprisingly among the first Omps whose 3D structure was solved at high resolution, namely, OmpF [12] and OmpC [13]. They show very high sequence identity (~60%) and virtually identical topology. Three identical subunits are arranged to form an homotrimer. Each monomer is folded as a 16-strands β-barrel pore,

where the longest loop L3 folds back and reduces water accessible area halfway through the channel. Thus, the lumen of each porin's monomer results in an hourglass shape, where the so-called constriction region generates the main steric barrier to the diffusion of molecules and ions.

For quite a long time, the reduced size and corresponding lower permeability of OmpC with respect to OmpF has lead to the convincing idea that pore size was the primary feature determining drugs permeability [6,10,14]. This concept was also corroborated by evidence of different level of expression for OmpF and OmpC depending on the environment and by the observation that mutant strains lacking OmpF and expressing OmpC showed decreased antibiotic susceptibility. Changes in medium osmolarity affect the relative expression of OmpC and OmpF, preferentially expressed in high and low osmolarity, respectively. Environments where nutrient levels are high, such as the mammal intestine, favor OmpC expression, when limitation of the influx of large and charged molecules such as bile salts and antibiotics is required; conversely, OmpF is the major porin under conditions of nutritional deficiency, when less stringent filtering is preferable [6].

Despite experimental and theoretical efforts spent during the last two decades [10,14–24], general rules for the design of novel drugs remain chimeric. Quite obviously, the focus of the studies has been typically the porin's constriction region. Different kinds of porin/antibiotic interactions have been invoked to explain permeability ranking, such as H-bonds, hydrophobic contacts and salt bridges. In some instances, the idea of a sort of binding or affinity site inside the channel has even loomed in the literature, in the search for a possible simple model to describe a clearly complex and multivariate process. The available results strongly suggest that permeation depends on general antibiotic physicochemical properties such as size, net charge, charge distribution, conformational plasticity and hydrophobicity, to name a few. Nevertheless, no evident strong correlation between the rates of permeation and any of these characteristics has been found so far, also for the lack of a robust method to measure permeability [25].

For the sake of completeness, it has to be mentioned that possible roles played by lipopolysaccharides (LPS) in the outer leaflet of the OM have been often underrated, if not completely neglected. The recent efforts spent in obtaining a reliable atomistic model for LPS simulations has revealed its non-passive role, with membrane thinning and direct interaction with the extracellular loops of the OM protein being just two examples of how the exact composition and flexibility of the OM itself can actually affect the behavior of the embedded protein [27–32].

More recently, the idea of strong direct interactions between the diffusing antibiotic and the channel residues has been questioned [10], and the electrostatics of the lumen, more than its size, has been indicated to be of primary importance in regulating permeability [14,19]. By using water molecules as inherent natural probes, the authors have characterized the internal electrostatics of OmpF, OmpC and some of its mutants [26] identified in clinical resistant strains [19]. The latter, isolated along two years of treatment of a patient suffering from a chronic *E. coli* infection, showed progressively greater resistance to the β-lactam antibiotics used for treatment, including cefotaxime, ceftazidime, ciprofloxacine, imipenem, and meropenem [27]. Interestingly, while the structures of the OmpC mutants showed essentially an unchanged size [19], remarkable differences were found in the electrostatics of OmpF, OmpC and the mutants [26]. All these porins share a constriction region with net segregation of oppositely charged residues. The loop L3 possesses several negatively charged residues, while the opposite side of the barrel wall is characterized by the presence of positively charged residues comprising the so-called 'basic ladder'. As expected, the internal electric field was found to be at the maximum in the constriction region, and this feature was absolutely invariant along the porin series investigated [26]. Conversely, major differences were found at the mouth of the constriction region on the extracellular side, and the existence of a 'pre-orientation region' has been put forward. Depending on the channel being considered, dipolar antibiotics might be effectively oriented in the pre-orientation region, resulting in a facilitated access to the constriction region [26].

A clear and systematic analysis of the role played by the channel in the translocation of antimicrobials, based on the knowledge of the dynamics of the translocating drugs themselves, is still missing [25]. There are no experimental methods available to probe the translocation directly. Computer simulations appear particularly suitable, if not necessary. After having characterized the internal electrostatics of the above mentioned series of porins in-depth, in the present work we have focused on the dynamics of antibiotics. By taking the unique opportunity of having the 3D structure of porins from progressively more resistant *E. coli* strains [19], we have selected two dipolar carbapenems to which resistance was assessed, namely, imipenem and meropenem. Recently, some of the authors have published a joint experimental and computational study where these two carbapenems have been compared [35]. A general decrease in the association rate through electrophysiology experiments, as well as a reduced permeability through liposome swelling assays, was observed for these two antibiotics along the series of OmpC mutants, thus, correlating with the decreased susceptibility observed in the clinical strains (35). In the present work, we have extended the computational investigation and

the analysis extent in order to characterize in much more details the new model for translocation we had put forward. In addition, some antibiotic-specific differences was shown but not fully understood (35). The free-energy profile of of imipenem and meropenem translocation through OmpF, OmpC, OmpC20 and OmpC33 (the first and the last one of the clinical series, respectively) was reconstructed through metadynamics simulations. The analysis of the permeation events shows how the antibiotic actually tries to align its electric dipole with the channel's electrostatics along its translocation path, and how even subtle differences between the channels can deeply affect the translocation process. In addition, the presented results clearly show that beside the channel-specific "background", the drug-specific properties do play a non negligible role in determining the dynamics of the translocation process.

Methods

We performed molecular dynamics simulations at an all-atom level on the four porins embedded in a POPC symmetric bilayer and solvated with water, as described in ref.[26], starting from their high-resolution X-ray structures (PDB Ids: 2OMF; 2J1N; 2XE2; 2XE3). The equilibrations were performed with the NAMD program. As interaction parameters we employed the Amber99SB-ILDN force field [28] for the protein and lipids, and TIP3P [29] for waters. All the amino acid residues were simulated in the ionization state at neutral pH except for the E296, which was protonated (net charge 0) as suggested for OmpF by Varma et al. [30].

We simulated the transport of antibiotics using an enhanced sampling technique, the well-tempered metadynamics algorithm [31], implemented in the ACEMD/PLUMED packages [32]. GAFF force-field parameters [33] were used to describe imipenem and meropenem, as described in details elsewhere [34]. Starting from the final configuration of the equilibrated porin simulation, the antibiotic was placed in the middle of the extracellular vestibule of the first monomer in a random orientation.

Two collective variables were biased, namely, the antibiotic position (z) and orientation inside the porin (supplementary figure S1), until the first translocation through the porin constriction region (0.0Å > z > -5.0Å) was observed. Then, four configurations were randomly selected, two with the antibiotic located in the extracellular vestibule, two in the periplasmic vestibule. Correspondingly, four multiple-walkers [35] were set to extend the metadynamics exploration of the free-energy surface (FES), reaching a total simulation time of 1.7-2.0 μs for each of the investigated cases. During the metadynamics stage, energy biases were added every 2.0 ps to each collective variable (the height of a single hill was 0.2 kcal mol^{-1}; the width was equal to 0.3 and 0.05 Å for position and orientation, respectively). For well-tempered scheme, we used

an initial height of the hills equal to 1.2 kcal mol^{-1}, modulated with a secondary temperature equal to 3000K. These biases discouraged the system from visiting conformations that had already been explored, thus enhancing the exploration of other states accessible to the system [31].

Results and discussion

Free Energy of Antibiotic Translocation: Serial Differences Do Not Focus on the Channel Constriction Zone

The free energy surface (FES) obtained for imipenem and meropenem while translocating through OmpF, OmpC, OmpC20 and OmpC33 are shown in figure 1. Antibiotic's depth inside the protein channel 'z' is reported on the y-axis: the constriction region encompasses the range between 0 and -5 Å and is highlighted in the figure. Antibiotic's orientation is reported on the x-axis: the closer to 0 the more perpendicular to the channel axis. The sign simply defines the two possible parallel orientations: a positive value corresponds to the antibiotic's positive part downward, i.e. closer to the periplasmic side. Thus, a change in the x-value on the FES represents the antibiotic reorienting inside the channel (supplementary Figure S1).

Along the minimum free energy path, different regions have been selected and analyzed in details (see below), in order to sample different portions of the channel in the range +10Å > z > -10Å. These regions are labeled with consecutive numbers in figure 1: moving from the extracellular to the periplasmic vestibule, the FES region's label increases. The highest free energy values are observed in the restricted central region in all the cases, in agreement with similar investigations reported in the literature [19,21,22]. However, the available space inside these four channels is known to be comparable [19], such that the differences observed in figure 1 cannot be explained with large variations of the steric hindrance to the antibiotic translocation.

A first analysis can be performed by comparing the FES relative to imipenem (figures 1a-1d). Constriction region accessibility from the periplasmic side is comparable in the four porins. On the other hand, constriction region accessibility from the extracellular side shows significant differences, when the average free energy level in the extracellular vestibule is compared to that at the constriction region in the same porin. In OmpF, the average ΔG is rather low all over the extracellular vestibule and starts to increase significantly from z=0Å, which is exactly where the constriction region starts. In OmpC, the main free energy barrier for translocation is broader, with ΔG significantly increasing already at z≈+5Å, meaning that accessibility to the core of the channel is less favorable than in OmpF [21]. In OmpC20, the main barrier is even

more pronounced and broad, with rather high free energy values starting from z≈+10Å, i.e. well outside the constriction region. Finally, in OmpC33, despite constriction region accessibility from the extracellular side looks ameliorated when compared to OmpC20, the main barrier to antibiotic diffusion is very broad and extends all the way from +10 to -5Å.

The case of meropenem follows the same trend (figure 1e-1h). Similarly to imipenem, the results for OmpF and OmpC are comparable each other, with constriction region accessibility being slightly less favorable in OmpC. In OmpC20, the main barrier for translocation is encountered well above the constriction region, clearly showing that in some circumstances the main difficulty might be approaching, more than crossing, the constriction region itself. In OmpC33, again, the central barrier is extremely broad, even more than observed for imipenem.

It is very interesting to note how the serial modifications observed along the channels series for both antibiotics pertain mostly to the area immediately above the constriction region (on the extracellular side) and not to the constriction region itself [26,36]. As already mentioned, all the four porins are comparable in size. In addition, the mutations differentiating them are not located in the constriction region [19], so that, similarly, an altered number of hydrogen bond donors/acceptors or charged groups in the constriction region cannot be invoked to explain the differences observed in the translocation FESs of each of the two carbapenems.

PORIN'S ELECTROSTATICS SETS THE SCENE: ROLE OF THE PRE-ORIENTATION REGION

We have recently characterized the subtle modifications of the charge distribution inside these protein channels [26]. Using water molecules as intrinsic and natural molecular probes for the electrostatics, the results suggested that the channel electrostatics might force dipolar molecules to adopt a pore-dependent preferential orientation while permeating through the channel. In addition, such a preferential orientation was found to vary along the channel, as if the channel directed a sort of choreography for molecules passing through it. The choreography is different for each porin in the series examined here, and ultimately depends upon the serial amino acid mutations evolved in the corresponding antibiotic resistant clinical strains [26,36].

It is thus plausible that antibiotics endowed with a significant electric dipole are forced to some extent to adopt a suitable orientation while translocating, in order to match the channel's electrostatics. As far as the latter is concerned, it has to be remarked that the most striking differences among the porins under investigation where found right at the mouth of the constriction region, on the extracellular side, which is exactly the same zone where the above described serial differences between the FESs have been found (figure 1).

This specific region corresponds to z values in the range from +10 to +5 Å in the systems discussed here and, by analogy with our previous report [26] it will be referred to as 'pre-orientation region'. This name was due to the differences observed between the four protein channels under investigation. It was shown that, in OmpF, waters' preferential orientation was almost the same as in the constriction region. The same direction was preserved also in OmpC but waters' ordering was lower, reflecting an attenuated (i.e. more balanced) electrostatics of the pre-orientation region. In OmpC20, waters' orientation in the pre-orientation region was inverted with respect to the constriction region. The same applied to OmpC33 to an even higher extent.

Figure 2 shows the xy-projection of the backbone of the porins' first monomer. For each of the labeled regions in figure 1, all the antibiotic conformers were extracted from Molecular Dynamics (MD) trajectories and analyzed by calculating the average electric dipole, which is reported in figure 2. In OmpF, imipenem does not change the orientation of its electric dipole while crossing the constriction region (figure 2a). The dipole is oriented from the basic ladder, which is positively charged, towards the loop L3, which is negatively charged, and this specific orientation was already adopted before entering the constriction region, when the antibiotic was still in the pre-orientation zone. Finally, upon emerging from the constriction region on the periplasmic side, the average orientation of the electric dipole changes by ~90°, as it was previously observed for waters [26].

In OmpC, the situation is rather different (figure 2b). Before entering into the constriction region, the electric dipole is not properly pre-oriented. Imipenem has to correct such a misalignment between its electric dipole and the channel electrostatics while crossing the constriction region. However, the change of dipole orientation is rather smooth, with ~90° variation covered along the path from region n.1 to n.3, while descending along the channel axis. Thus, finally, imipenem adopted the correct orientation in the constriction region. Afterwards, an additional ~90° variation upon emerging to the periplasmic vestibule is observed, similarly to the case of OmpF.

In OmpC20, the adverse pre-orientation above the constriction region is absolutely clear (figure 2c). Imipenem has to rotate its dipole while descending along the channel in less than 1 nm (from region n.1 to n.3) in order to reach the correct alignment before getting into the most restricted zone. Finally, in OmpC33, the changes in the orientation of the dipole appear even sharper than in the case of OmpC20 (figure 2d). Dipole orientation abruptly changes by ~180° both getting in and out of the constriction region, and it is not properly oriented even inside the constriction region.

The case of meropenem follows the same trend, bolstering the primary role played by channel electrostatics as a background for the antibiotic's translocation choreography. The analysis of the FES' selected regions along the minimum energy path shows that, in OmpF, the pre-orientation exerted by the electrostatics at the extracellular mouth of the constriction region is such that meropenem can enter the constriction region with just a slight change of orientation (figure 2e). In OmpC, the change of orientation is larger but rather smooth while traversing the channel (figure 2f). In OmpC20, the pre-orientation is strong and points ~180° away from the optimal direction to get into the constriction region (figure 2g). An inversion of the molecular dipole orientation is needed while descending only 1-2 nm along the translocation path. Finally, in OmpC33, the adverse pre-orientation is clear and, in addition, the antibiotic seems to never reach the proper orientation inside the constriction region (figure 2h).

From this qualitative analysis it is clear that both carbapenems, being highly dipolar molecules (14 and 31 D respectively for imipenem and meropenem [34]), are forced to adopt specific orientations along their way through the porin, in perfect agreement with our previous water analysis [26]. The drug possessing a dipole is effectively pre-oriented in OmpF at the level of the extracellular vestibule, that is, before entering the constriction region. This results in a very good accessibility of the constriction region from the extracellular side. In OmpC, pre-orientation is not effective, so that the dipolar drug has to find the proper orientation without any "guide" from the channel electrostatics. In the case of the two clinical mutants, OmpC20 and OmpC33, the pre-orientation acts in the opposite direction with respect to the electrostatics in the constriction region, dramatically reducing the probability for the antibiotic to access the latter properly, i.e. with the optimal orientation of its electric dipole.

Zooming In for a Close-Up of Antibiotic Reorientations

The curved lines in Figure2 show qualitatively the progressive variation of the dipole orientation inside the pore, correlated to the reorientation of the dipolar drug, moving from OmpF to OmpC and than for the two pores extracted from clinical strains. In order to get a more detailed and quantitative description of the reorientations executed by the two carbapenems inside the four channels, we performed a statistical analysis of the polar coordinates of the electric dipole. By taking into account all the MD frames pertaining to adjacent cross-sections of the channels with 2.5Å width, we computed the distribution of the azimuth and altitude angles, as defined in figure 3a. Figure 3b shows the azimuth of waters' net dipole, in the absence of any antibiotic, as a reference.[§] OmpF and OmpC are absolutely comparable from this point of view, the only difference is the magnitude of the xy-component

of the waters' net dipole (not shown), which is strong in OmpF whereas almost absent in OmpC [26]. In OmpC20, the pre-orientation is opposite to the waters' order observed in the constriction region, but follows a smooth variation along the channel axis. In OmpC33, the adverse pre-orientation is retained deeper inside the channel and the dipole orientation is forced to change when the antibiotic is closer to the constriction region, i.e. where the available space is reduced.

As far as the two carbapenems' choreography is concerned, the altitude was never found to follow any specific and informative trend, which is absolutely reasonable given the rather small z-component of waters' net dipole when compared to the xy-component. On the other hand, the azimuth was found to be a clear descriptor for the differences in the behavior of the same antibiotic into the various porins. In figure 4, the results for imipenem are shown for two selected cross-sections, one in the pre-orientation and one in the constriction region, respectively. The corresponding full figure S2 can be found in the supplementary material on-line. In OmpF, imipenem descends from the pre-orientation to the constriction region with the electric dipole pointing towards the same direction. The main fraction of conformers populates the portion of the azimuth domain closest to the reference waters' net dipole in the same cross-section. When imipenem enters the region of the channel with the lowest accessible area, molecular reorientations are hindered. The azimuth distribution reflects the reduced interchangeability between different orientations by a broader and more complex profile. Figure 5 shows, for instance, the centroid of three different clusters of molecular conformers, sampled from the azimuth distribution in the constriction region.

In OmpC, where pre-orientation is not effective, the azimuth distributions are broader than observed in OmpF, for every cross-section between the pre-orientation and the constriction region (figures 4 and S2). There is not one clear main fraction of conformers properly aligned to the channel electrostatics, showing that imipenem is not driven to adopt any specific orientation along its way towards the constriction region.

The case of OmpC20 might be misleading at a first sight. The azimuth distributions clearly show that the electrostatics at the pre-orientation region is absolutely effective. By virtue of the large variation of directionality in the following cross-sections, imipenem is not able to properly follow the electrostatics variations while descending towards the constriction region. Nevertheless, quite surprisingly, the azimuth distribution in the constriction region results very well centered around the "correct" orientation (figure 4 and S2).

In order to discern this apparent discrepancy, it has to be noted that the azimuth distributions do not take the magnitude of the dipole xy-projection into any account. It is important to focus on

the entropic nature of the main barrier for antibiotic translocation through the general porins under investigation [15,17,21,23,24,37,38]. The unfavorable entropic cost coming from desolvation and confinement of the drug inside the constriction region can be (partially) compensated by favorable drug-porin interactions, like H-bonds and salt bridges. In this scenario, where entropy-enthalpy balance is crucial, the optimal alignment of the antibiotic's electric dipole to the channel electrostatics comes into play.

Figure 6 shows different conformers, which were all extracted from the main population of the azimuth distribution of imipenem's dipole in the constriction region of OmpC20, as representative structures for different conformational clusters actually pertaining to the same azimuth population. The optimal molecular orientation was sometimes observed (figure 6b), where the magnitude of the xy-component of the dipole is close to the maximum value achievable; however, imipenem was often found either to be extended but mostly oriented along the channel axis (figure 6c and 6d), or to assume a compact scorpion-like conformation with a reduced electric dipole (figure 6e and 6f). All of these conformers are characterized by a significantly lower xy-component of the dipole moment than the one depicted in figure 6b, meaning that the energy gain coming from dipole alignment to the channel electrostatics is proportionally lower.

A comprehensive picture was obtained by calculating the cross-correlation between the azimuth distribution and the xy-magnitude of the electric dipole. Results are shown in figure S3. The agreement between these results and the qualitative argumentation on the constriction region accessibility discussed above (figure 1) is remarkable. In OmpF, the highest probability is found for a good azimuthal alignment of the drug's dipole (around 0 degree) and rather high values of the xy-magnitude (>20 D). In OmpC, the ineffective pre-orientation translates into an increased disorder of the antibiotics' dipole orientation inside the constriction region. In figure S3, a broader distribution with a significant probability for wrong orientations can be clearly seen for this protein. In OmpC20, despite the distribution of the azimuth is as narrow as in OmpF, the distribution of the xy-magnitude is broader, reaching values as low as ~10 D with a rather high probability. In the extracellular vestibule, the antibiotic is pre-oriented in the opposite direction to the one needed to get into the constriction region and should reorient while translocating by just ~1 nm. As a result, it often assumes non-optimal conformations when entering the constriction region (figure 6), thus loosing the benefits from an optimal alignment of the electric dipole to the pore's electrostatics. Finally, in OmpC33, the combination of an effective adverse pre-orientation and the fact that such pre-orientation is kept

deeper into the channel (figure 3), leads to a dramatic increase of the probability to obtain a misalignment of the dipole inside the constriction region (figure S3).

In figure S4, meropenem choreography in the four protein channels is compared. The overall trends and the differences are absolutely comparable to the case of imipenem. These results clearly points to the major role played by the electrostatics of the channel in driving the reorientations and, thus, the translocation path of dipolar antibiotics like the two carbapenems investigated in this work. In figure S5, the cross-correlation between the azimuth and xy-magnitude of the electric dipole is shown for meropenem in the constriction region of the four porins, providing a more comprehensive picture than the one offered by simple azimuth distributions.

In OmpF, the highest probability is found for good azimuthal alignment (around 0 degree) and high values of the xy-projection (around 30 Debye). In OmpC, the highest probability is similarly found for good azimuthal alignment but at a significantly lower xy-magnitude. In addition, the two-dimensional probability distribution is more asymmetric than observed for OmpF in both dimensions. Along the xy-magnitude, the tail on the high values side has almost completely disappeared moving from OmpF to OmpC. Along the azimuth angle, the probability for negative deviations from the reference value obtained from water ordering has significantly increased. In the case of OmpC20, the deviation from the optimal alignment is clear. Finally, in OmpC33, similarly to the case of imipenem, the combination of an effective adverse pre-orientation, and the fact that this is kept deeper into the channel, leads to a dramatic increase of the probability for dipole misalignment from channel electrostatics inside the constriction region.

Antibiotic-Specific Features Come Into Play on the Porin's Choreography

Beside the porin-dependent "background", a deeper inspection of our results suggests important antibiotic-specific differences playing their role. The shorter and more flexible imipenem actually appears more sensitive to the pre-orientation. A generally more disordered population of conformers was found, indeed, when moving from one porin to the next along the series presented in this work. On the other hand, the longer and more rigid meropenem does not follow pre-orientation with the same accuracy as that of imipenem, since its reorientations are hindered already in the extracellular vestibule due to the larger size of this antibiotic. In addition, the positively charged group of meropenem is not located at the end of a flexible side chain like in imipenem, but on a rigid ring separated by only two rotatable bonds from the carboxyl group. The combination of these molecular features is reflected by a generally less

disordered distribution of the electric dipole orientation inside the constriction region. Indeed, despite meropenem adopts different conformations, the azimuth and the xy-magnitude of its electric dipole are far less dependent from side chain fluctuations than they are in the case of imipenem. For instance, figure 7 shows different conformers of meropenem in the constriction region of OmpC20. All of these are representative structures of different conformational clusters.

Finally, aiming at capturing all of these molecular features in a unique parameter, figure 8 compares the distributions of the dipole modulus and the angle between the dipole itself and the main molecular axis of inertia, obtained for all the investigated cases when the antibiotic is located inside the constriction region. The corresponding results obtained in bulk water (ad hoc MD simulations were performed with just the antibiotic in a water box) are also shown for the sake of comparison. No significant variation of the modulus of the electric dipole is observed in the different porins and when compared to the distribution in bulk water. Meropenem, on average, shows higher values than imipenem. On the other hand, more interesting differences are observed when the angle between the dipole and the main molecular axis is compared. In agreement with all of the results and comparisons shown above, OmpF (figure 8f) does not impose the two antibiotics to populate conformations that are not inherently populated in bulk water (figure 8j). As far as the electric dipole deviation from the main molecular axis is concerned, imipenem and meropenem appear fairly comparable in this case. However, looking at OmpC and its mutants, in the case of meropenem, such molecular feature is scarcely influenced by the specific porin being crossed, and the obtained distributions are comparable to each other and to the one in bulk water. Conversely, imipenem results deeply affected by the porin, as it populates conformations characterized by a larger dipole-main axis deviation, whose probability increases along the series OmpC, OmpC20 and OmpC33.

Conclusions

The similarities observed in the behavior of the two carbapenems investigated here show the major role played by the specific porins under consideration. The characteristic hourglass shape of these general unspecific channels dictates the presence of a main barrier for the translocation of metabolites and drugs, which is basically entropic. Differences in the electrostatics of the four channels result in impressive changes of the orientations assumed by dipolar molecules during the passage, as shown in the present work by comparing the translocation path of the

same carbapenems through different porins. The effects of the electrostatics appear so large that in some cases it is more difficult for the drug to approach, rather than enter, the channel's constriction region, as observed for the two OmpC mutants from *E. coli* resistant strains.

Nevertheless, a deeper inspection and careful comparison of the results we have shown, suggested that important antibiotic-specific differences apply on the porin-dependent "background". The shorter and more flexible imipenem appeared more sensitive to the effects of a different pre-orientation. On the other hand, the longer and more rigid meropenem did not follow pre-orientation with the same accuracy as that of imipenem.

Interestingly, as a concluding remark, a closer look at the distributions obtained in bulk water reveals that an inherently different propensity towards large deviations between the direction of the electric dipole and the main molecular axis of inertia actually exists among these two carbapenems. In our opinion, the latter represents an intrinsic antibiotic-specific feature deserving particular attention in the future for a more rational drug design. By taking multiple molecular "classic" parameters into account, being probably more important than the simple size, net charge, conformational plasticity, etc…, it appears fundamental in determining the overall permeability through the target porin.

A concluding remark has also to be devoted to the membrane model employed here. Although certainly useful to compare our theoretical results to a variety of experimental setups, the overall permeability of dipolar molecules through OM porins is not only due the phenomena described in the present work. For instance, MD simulations of the TonB-dependent transporter FecA both within symmetric phosholipid bilayer and asymmetric phospholipid/LPS bilayer have shown how the extracellular loops of the embedded protein channel can interact with the LPS [46]. These interactions might result in significant differences of both local fluctuations as well as larger conformational motions of the protein loops, ultimately affecting permeability and transport properties [46]. Thus, the aspects investigated in the present work, focused on the dynamics of the crossing drug in response to the internal electrostatics of the channel, are hardly affected by the plasticity of the extracellular loops, but the latter may be among the main determinant for the overall permeability and surely deserves detailed investigations towards a comprehensive picture of the dipolar antibiotics' translocation across the OM.

Future Perspectives

To understand how porins located in the outer membrane of Gram-negative bacteria are able to filter noxious molecules is extremely important to design/optimize new antibacterials with better permeation. In this context, the availability of high-resolution crystal structures is

fundamental to unveil the molecular mechanism of filtering in bacterial porins. The level of sophistication of modern molecular modeling algorithms together with the employment of new computer hardware makes it possible to simulate these complex processes at the molecular level of detail. Our recent efforts have shown that a synergistic combination of structural data, in vitro assays and computer simulations is capable to come to a real identification and description of the physical and chemical properties of molecules that can cross the outer membrane barrier. Once the "golden rules" of permeation will be fully understood, the application of virtual screening techniques will help to search for new scaffolds with enhanced permeation, with molecular modeling being extremely helpful for compounds optimization.

Executive Summary

- The analysis of molecular dynamics trajectories revealed how dipolar antibiotics reorient inside bacterial porins to match the channel's electrostatics.
- The analysis of a series of clinical resistant mutants showed modifications in the so-called pre-orientation region as key for the antibiotic translocation path
- The importance of proper alignment of the molecular dipole during the translocation has been highlighted and the deviation of dipole direction from the main molecular axis of inertia has been put forward as a parameter for drug design

Footnotes

[§]The azimuth found in the cross-section with the highest waters order was used as angular reference and thus placed to zero. Data pertaining to the other cross-sections, both in the presence and absence of the antibiotic, were phased accordingly.

References

1. Brown ED, Wright GD. Antibacterial drug discovery in the resistance era. *Nature*. 529(7586), 336–343 (2016).

2. Tommasi R, Brown DG, Walkup GK, Manchester JI, Miller AA. ESKAPEing the labyrinth of antibacterial discovery. *Nat. Rev. Drug Discov.* 14(8), 529–542 (2015).

3. When the drugs don't work. *Nat. Microbiol.* 1(2), 16003 (2016).

4. WHO. Antimicrobial resistance: global report on surveillance [Internet]. World Health Organization Available from: http://www.who.int/drugresistance/documents/surveillancereport/

en/.

5. Wright GD. The antibiotic resistome: the nexus of chemical and genetic diversity. *Nat. Rev. Microbiol.* 5(3), 175–186 (2007).

6. Masi M, Pagès J-M. Structure, Function and Regulation of Outer Membrane Proteins Involved in Drug Transport in Enterobactericeae: the OmpF/C – TolC Case. *Open Microbiol. J.* 7, 22–33 (2013).

7. Lewis K. Platforms for antibiotic discovery. *Nat. Rev. Drug Discov.* 12(5), 371–387 (2013).

8. Isabella VM, Campbell AJ, Manchester J, *et al.* Toward the Rational Design of Carbapenem Uptake in Pseudomonas aeruginosa. *Chem. Biol.* 22(4), 535–547 (2015).

9. Delcour AH. Outer membrane permeability and antibiotic resistance. *Biochim. Biophys. Acta BBA - Proteins Proteomics*. 1794(5), 808–816 (2009).

10. Kojima S, Nikaido H. Permeation rates of penicillins indicate that Escherichia coli porins function principally as nonspecific channels. *Proc. Natl. Acad. Sci.* 110(28), E2629–E2634 (2013).

11. Pagès J-M, James CE, Winterhalter M. The porin and the permeating antibiotic: a selective diffusion barrier in Gram-negative bacteria. *Nat. Rev. Microbiol.* 6(12), 893–903 (2008).

12. Cowan S, Schirmer T, Rummel G, *et al.* Crystal-Structures Explain Functional-Properties of 2 Escherichia-Coli Porins. *Nature*. 358(6389), 727–733 (1992).

13. Baslé A, Rummel G, Storici P, Rosenbusch JP, Schirmer T. Crystal Structure of Osmoporin OmpC from E. coli at 2.0 Å. *J. Mol. Biol.* 362(5), 933–942 (2006).

14. Kojima S, Nikaido H. High Salt Concentrations Increase Permeability through OmpC Channels of *Escherichia coli*. *J. Biol. Chem.* 289(38), 26464–26473 (2014).

15. Tran Q-T, Williams S, Farid R, Erdemli G, Pearlstein R. The translocation kinetics of antibiotics through porin OmpC: Insights from structure-based solvation mapping using WaterMap. *Proteins Struct. Funct. Bioinforma.* 81(2), 291–299 (2013).

16. Brown DG, May-Dracka TL, Gagnon MM, Tommasi R. Trends and Exceptions of Physical Properties on Antibacterial Activity for Gram-Positive and Gram-Negative Pathogens. *J. Med. Chem.* 57(23), 10144–10161 (2014).

17. Ziervogel BK, Roux B. The Binding of Antibiotics in OmpF Porin. *Structure*. 21(1), 76–87 (2013).

18. Raj Singh P, Ceccarelli M, Lovelle M, Winterhalter M, Mahendran KR. Antibiotic Permeation across the OmpF Channel: Modulation of the Affinity Site in the Presence of Magnesium. *J. Phys. Chem. B.* 116(15), 4433–4438 (2012).

19. Lou H, Chen M, Black SS, *et al.* Altered Antibiotic Transport in OmpC Mutants Isolated from a Series of Clinical Strains of Multi-Drug Resistant E. coli. *PLoS ONE*. 6(10), e25825 (2011).

20. O'Shea R, Moser HE. Physicochemical Properties of Antibacterial Compounds: Implications for Drug Discovery. *J. Med. Chem.* 51(10), 2871–2878 (2008).

21. Kumar A, Hajjar E, Ruggerone P, Ceccarelli M. Molecular Simulations Reveal the Mechanism and the Determinants for Ampicillin Translocation through OmpF. *J. Phys. Chem. B.* 114(29), 9608–9616 (2010).

22. Mahendran KR, Hajjar E, Mach T, *et al.* Molecular Basis of Enrofloxacin Translocation through OmpF, an Outer Membrane Channel of Escherichia coli - When Binding Does Not Imply Translocation. *J. Phys. Chem. B.* 114(15), 5170–5179 (2010).

23. Danelon C, Nestorovich EM, Winterhalter M, Ceccarelli M, Bezrukov SM. Interaction of Zwitterionic Penicillins with the OmpF Channel Facilitates Their Translocation. *Biophys. J.* 90(5), 1617–1627 (2006).

24. Hajjar E, Bessonov A, Molitor A, *et al.* Toward Screening for Antibiotics with Enhanced Permeation Properties through Bacterial Porins. *Biochemistry (Mosc.)*. 49(32), 6928–6935 (2010).

25. Winterhalter M, Ceccarelli M. Physical methods to quantify small antibiotic molecules uptake into Gram-negative bacteria. *Eur. J. Pharm. Biopharm.* 95, 63–67 (2015).

26. Acosta-Gutierrez S, Scorciapino MA, Bodrenko I, Ceccarelli M. Filtering with Electric Field: The Case of *E. coli* Porins. *J. Phys. Chem. Lett.* 6(10), 1807–1812 (2015).

27. Low AS, MacKenzie FM, Gould IM, Booth IR. Protected environments allow parallel evolution of a bacterial pathogen in a patient subjected to long-term antibiotic therapy. *Mol. Microbiol.* 42(3), 619–630 (2001).

28. Lindorff-Larsen K, Piana S, Palmo K, *et al.* Improved side-chain torsion potentials for the Amber ff99SB protein force field. *Proteins*. 78, 1950–1958 (2010).

29. Jorgensen W, Chandrasekhar J, Madura J, Impey R, Klein M. Comparison of simple potential functions for simulating liquid water. *J. Chem. Phys.* 79, 926–936 (1983).

30. Varma S, Chiu S-W, Jakobsson E. The Influence of Amino Acid Protonation States on Molecular Dynamics Simulations of the Bacterial Porin OmpF. *Biophys. J.* 90(1), 112–123 (2006).

31. Barducci A, Bussi G, Parrinello M. Well-Tempered Metadynamics: A Smoothly Converging and Tunable Free-Energy Method. *Phys. Rev. Lett.* 100(2), 020603 (2008).

32. Harvey M, Giupponi G, De Fabritiis G. ACEMD: Accelerating Biomolecular Dynamics in the Microsecond Time Scale. *J. Chem. Theory Comput.* 5, 1632–1639 (2009); Bonomi M, Branduardi D, Bussi G, Camilloni C, Provasi D, Raiteri P, Donadio D, et al.: PLUMED: a

Portable Plugin for Free-Energy Calculations with Molecular Dynamics. *Comp Phys Comm* 180, 1961–72 (2009).

33. Wang J, Wolf RM, Caldwell JW, Kollman PA, Case DA. Development and testing of a general amber force field. *J. Comput. Chem.* 25(9), 1157–1174 (2004).

34. Malloci G, Vargiu AV, Serra G, Bosin A, Ruggerone P, Ceccarelli M. A Database of Force-Field Parameters, Dynamics, and Properties of Antimicrobial Compounds. *Molecules.* 20(8), 13997–14021 (2015).

35. Raiteri P, Laio A, Gervasio FL, Micheletti C, Parrinello M. Efficient reconstruction of complex free energy landscapes by multiple walkers metadynamics. *J. Phys. Chem. B*. 110(8), 3533–3539 (2006).

36. Bajaj H, Scorciapino MA, Moynié L, *et al.* Molecular Basis of Filtering Carbapenems by Porins from β-Lactam-resistant Clinical Strains of *Escherichia coli*. *J. Biol. Chem.* 291(6), 2837–2847 (2016).

37. Ceccarelli M, Vargiu AV, Ruggerone P. A kinetic Monte Carlo approach to investigate antibiotic translocation through bacterial porins. *J. Phys. Condens. Matter*. 24(10), 104012 (2012).

38. D'Agostino T, Salis S, Ceccarelli M. A kinetic model for molecular diffusion through pores. *Biochim. Biophys. Acta*. (2016).

Figure 1. Free energy surface of the translocation of imipenem **(a-d)** and meropenem **(e-h)** through four different outer membrane porins from *E. coli*. The wild-type OmpF **(a,e)** and OmpC **(b,f)** together with mutants OmpC20 **(c,g)** and OmpC33 **(d,h)** from clinical strains have been investigated. Each isocontour corresponds to a free energy difference of 2 kcal mol^{-1}. Free energy values were rescaled for each surface in order to have the absolute minimum equal to zero. Numerical labels are used to indicate specific regions analyzed in details along the minimum energy path across the constriction region, whose boundaries are highlighted with red lines (0Å < z < -5Å).

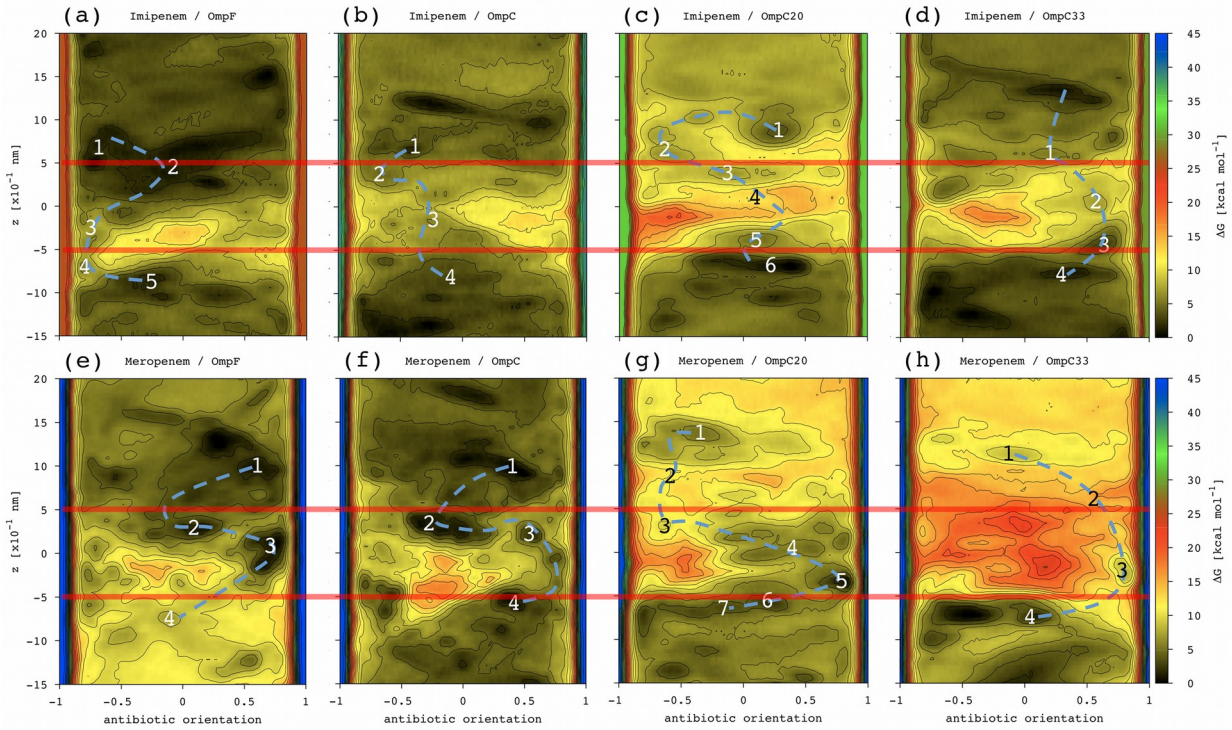

Figure 2. Backbone xy-projection of the first monomer of the four different outer membrane porins from *E. coli*, namely, the wild-type OmpF **(a,e)** and OmpC **(b,f)** together with mutants OmpC20 **(c,g)** and OmpC33 **(d,h)** from clinical strains. The loop L3 is bolded to provide a visual reference. The dashed line is used to indicate the optimal direction for molecular dipoles inside the constriction region.[26] The average projection on the xy plane of the electric dipole of imipenem **(a-d)** and meropenem **(e-h)** in each of the labeled regions of the corresponding FES in figure 1, are reported with different colors. The curved lines represent the maximum reorientation of the dipole moment experienced by each antibiotic during the passage.

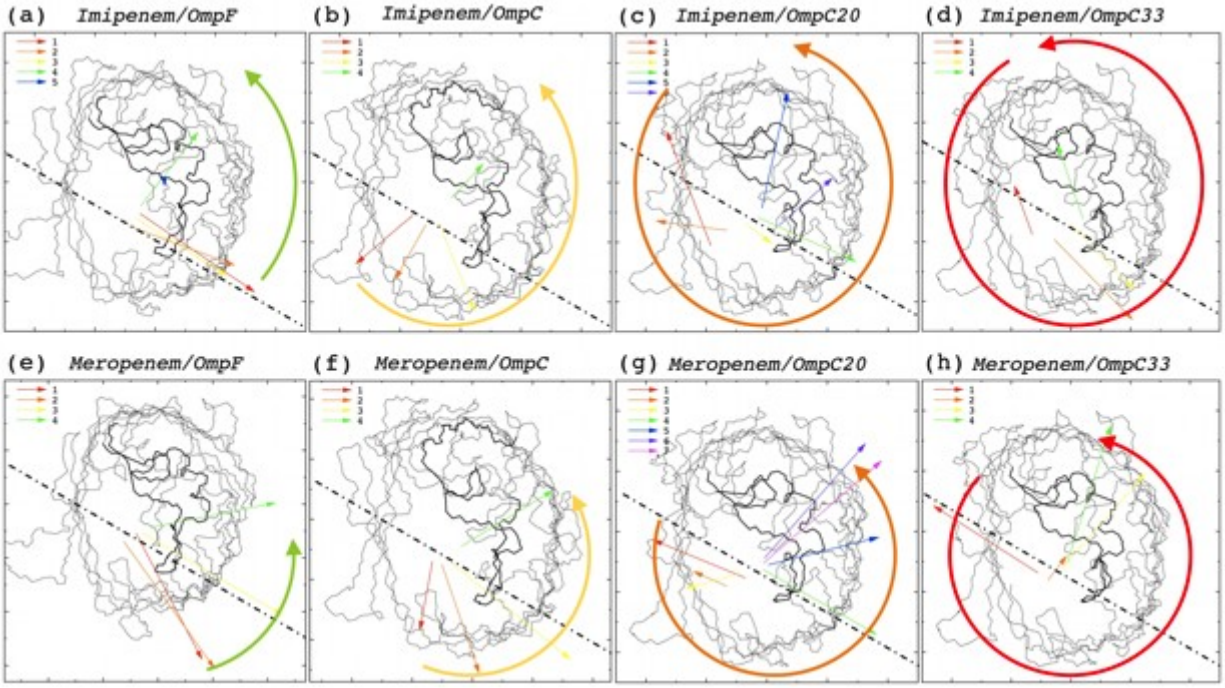

Figure 3. Electric dipoles orientation was analyzed in terms of polar coordinates as defined in **(a)**. In **(b)**, the results of the azimuth angle of the waters' net dipole in the absence of antibiotic are reported for successive 2.5Å cross-sections along the channel axis of the four porins under investigation. The shaded area indicates the constriction region.

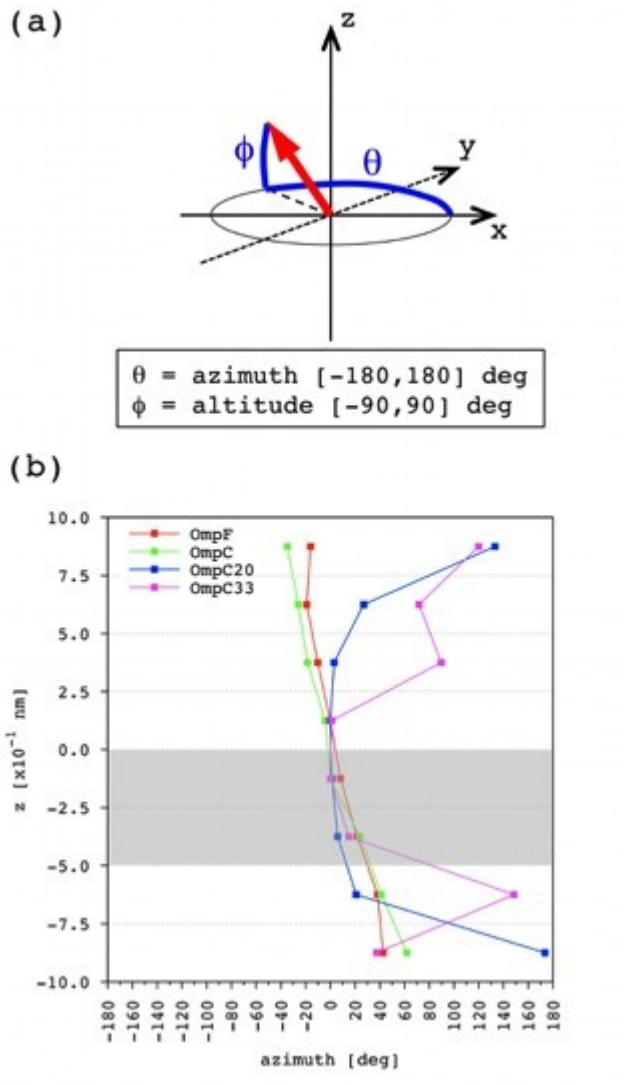

Figure 4. The distribution of the azimuth angle of imipenem's electric dipole is shown for two selected 2.5Å cross-sections along the channel axis of the four outer membrane porins under investigation. The first cross-section (+10.0Å < z < +7.5Å) is in the pre-orientation region, the second one (0.0 Å < z < -2.5Å) is in the constriction region of the pore. The red lines are used as a reference for the azimuth of the waters' net dipole in the same channel cross-section, calculated in the absence of antibiotic.

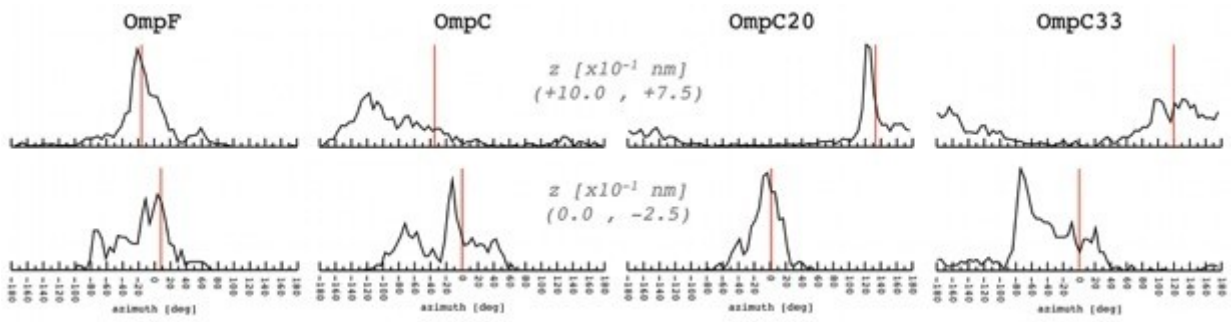

Figure 5. The distribution of the azimuth angle of imipenem's electric dipole at the constriction region of OmpF is shown **(a)**. The three shaded regions highlight the corresponding populations sampled (red, closest to the waters' net dipole; green, acceptable alignment; blue, severely misaligned). In **(b)**, the centroid of the three corresponding antibiotic clusters are color coded in agreement to **(a)**, and are shown inside the cartoon of the 3D structure of the porin's monomer, where only loop L3 is colored to provide a reference.

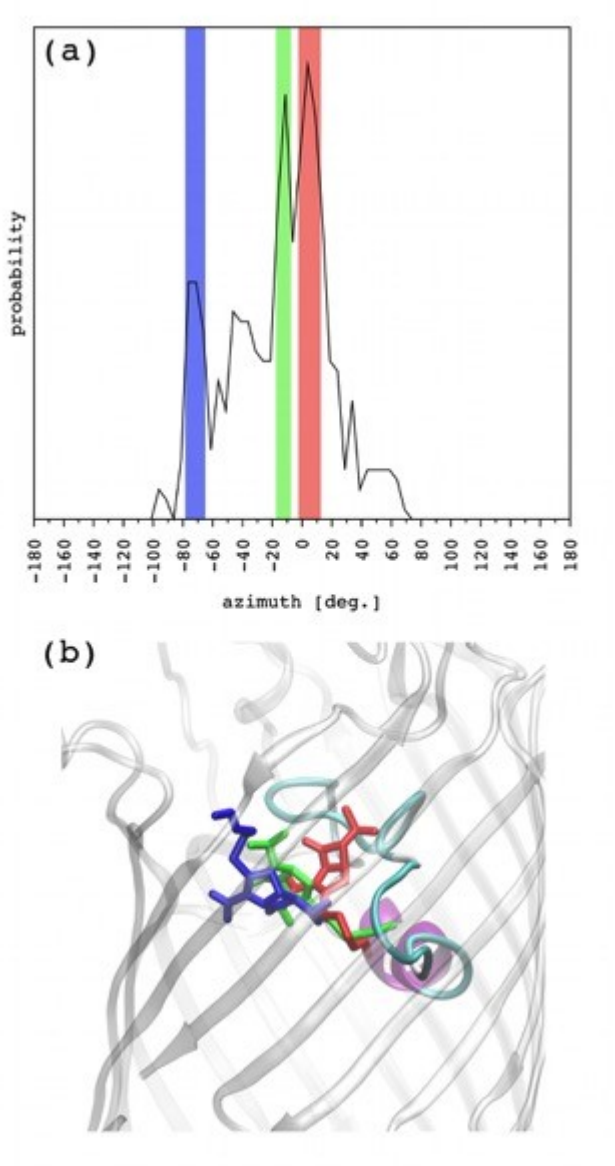

Figure 6. The distribution of the azimuth angle of imipenem's electric dipole in the constriction region of OmpC20 is shown **(a)**. The red shaded region highlights the corresponding population sampled (the main one and closest to the waters' net dipole). In **(b-f)**, different conformers of imipenem are shown, chosen as being representative for different conformational clusters pertaining to the same azimuth population highlighted in **(a)**. These are shown inside the cartoon of the 3D structure of the porin's monomer, where only loop L3 is colored to provide a reference. The green dashed arrows are used to indicate the dipole's orientation.

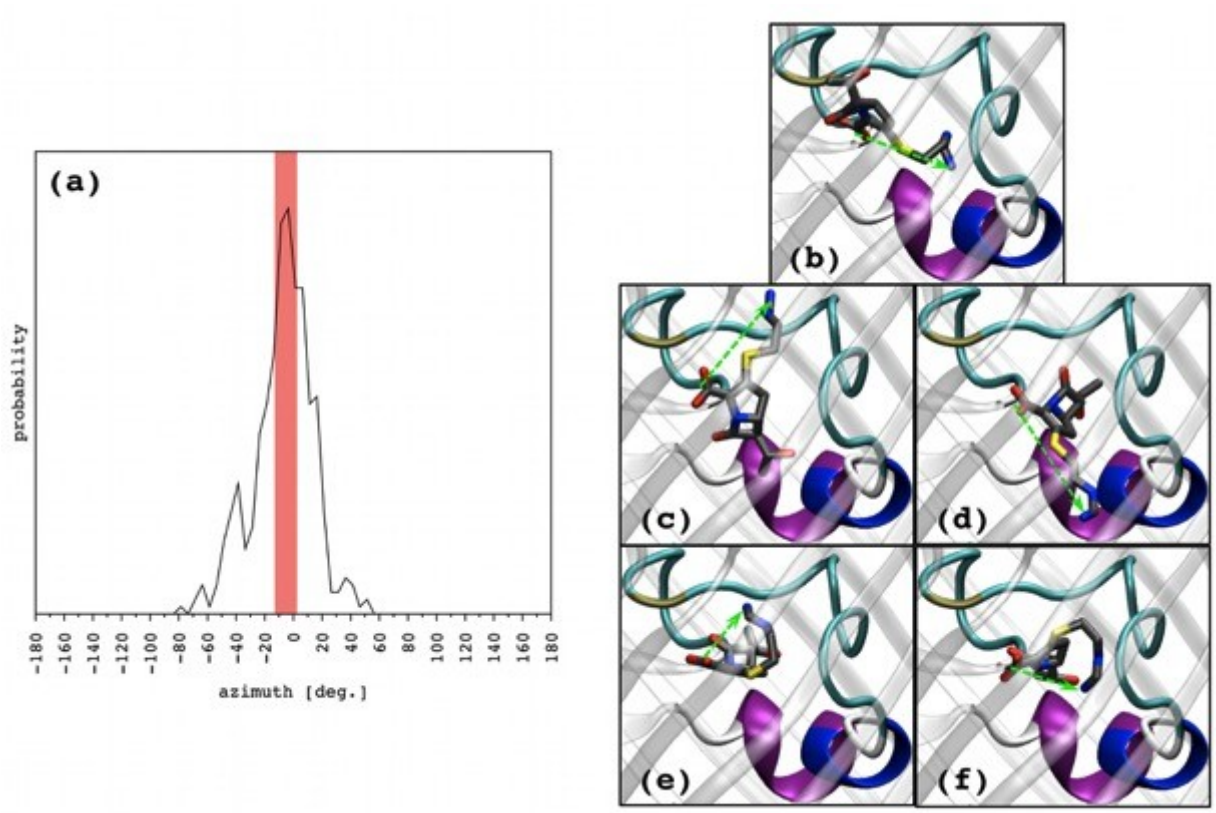

Figure 7. Different conformers of meropenem are shown, chosen as being representative for different conformational clusters in the constriction region of OmpC20. They are shown inside the cartoon of the 3D structure of the porin's monomer, where only loop L3 is colored to provide a reference. The green dashed arrows are used to indicate the dipole's orientation.

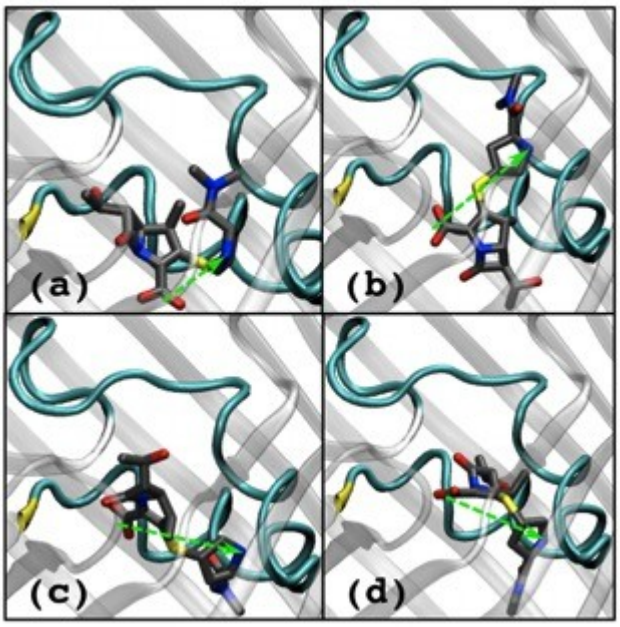

Figure 8. The distribution of the dipole modulus **(a-e)** is shown together with the distribution of the plain angle between the electric dipole itself and the main axis of inertia **(f-j)** for imipenem (red) and meropenem (blue) inside the constriction region of the four porins under investigation, as well as in bulk water for the sake of comparison.